INT. J. ELECTRONICS,
VOL. 91, NO. 11, NOVEMBER 2004, 639–651

Hysteresis current control of a vector controlled induction motor and DTC: an assessment

J. RODRÍGUEZ†, J. PONTT†, C. SILVA†, S. KOURO†*, A. LIENDO† and J. REBOLLEDO†

This paper presents the speed control of an induction motor using nonlinear current control in rotating coordinates. Two hysteresis comparators and the position of the motor flux are used to generate directly the gate pulses for the power transistors of the inverter. This field oriented control method is compared with direct torque control and it is concluded that both control methods, although being conceptually different, have very similar features in terms of structure and performance. Experimental results confirm the high quality of the control reached with this control strategy.

Nomenclature

Y_i	conduction state of transistor i
$\mathbf{V}_1 \ldots \mathbf{V}_6$	voltage vectors generated by the inverter
$\mathbf{v}_s$	stator voltage space vector
$\mathbf{i}_s$	stator current space vector
$\boldsymbol{\psi}_r$, $\boldsymbol{\psi}_s$	rotor and stator flux space vectors
σ	induction machine leakage coefficient
L_m, L_s and L_r	magnetizing, stator and rotor inductance
R_r, R_s	rotor and stator resistance
ω_2, ω_{syn}	slip and synchronous frequency
ω_r	induction machine rotational speed
p	number of pole pairs
T_e	electrical torque
θ_{syn}	position of rotor flux
θ_s	position of the stator flux
V_c	DC link voltage
δ	hysteresis band
h_d, h_q, h_T, h_ψ	hysteresis outputs
ε	control error
$*$	reference value
r, s	rotor and stator quantities
(α, β)	stator fixed coordinates
(d, q)	synchronous rotating coordinates
(a, b, c)	motor three-phase variables

Received 19 January 2004. Accepted 13 November 2004.
*Corresponding author. e-mail: samir.kouro@elo.utfsm.cl
†Electronics Department, Universidad Técnica Federico Santa María, Av. España 1680, Casilla 110-V, Valparaíso, Chile.

International Journal of Electronics ISSN 0020–7217 print/ISSN 1362–3060 online
http://www.tandf.co.uk/journals
DOI: 10.1080/00207210412331332871

1. Introduction

Direct torque control (DTC) was introduced in the literature during 1985–1986 (Takahashi and Noguchi 1986, Depenbrock 1988) and in the industry in the 1990s (Tiitinen *et al.* 1995). Today DTC is recognized as a high performance control method for AC machines, allowing for fast torque control. In addition, DTC is very interesting and attractive from a conceptual point of view, because it integrates directly and clearly the power circuit of the inverter and the gate drive pulses generation with the behaviour of torque and flux in the machine. For this reason, almost all modern books on electrical drives include a special chapter dedicated to DTC (Vas 1998, Boldea and Nasar 1999, Mohan 2001, Trzynadlowski 2001, Kazmierkowski *et al.* 2002). Today, it is considered that the most attractive features of DTC in relation to classical field oriented control are (Boldea and Nasar 1999, Trzynadlowski 2001):

- DTC does not need an additional modulator.
- DTC does not need to tune current controllers.

This paper presents a nonlinear current control method for a vector controlled induction motor having very similar properties compared to DTC: it does not need a modulator or adjustment of linear controllers. The control strategy was originally conceived using the principle of field orientation and applied to inverter and matrix converter-fed induction machines (Rodríguez and Kastner 1985, 1987). The following sections present the fundamentals of the control strategy, the pulses generation, experimental results and a comparison to DTC.

2. The inverter

2.1. *Topology*

Figure 1 shows the power circuit of a three-phase voltage source two level inverter and the stator circuit of the induction machine. Let the binary variables $Y_1, Y_2, \ldots, Y_6$ represent the conduction state of each transistor, i.e. if $Y_k = 1$, then T_k is conducting and if $Y_k = 0$, then T_k is not conducting, for $k \in \{1, 2, \ldots, 6\}$.

In this topology only one transistor per leg is conducting at any time, i.e. $Y_{2k} = 1 - Y_{2k-1}$, for $k = \{1, 2, 3\}$. For this reason, the inverter state can be

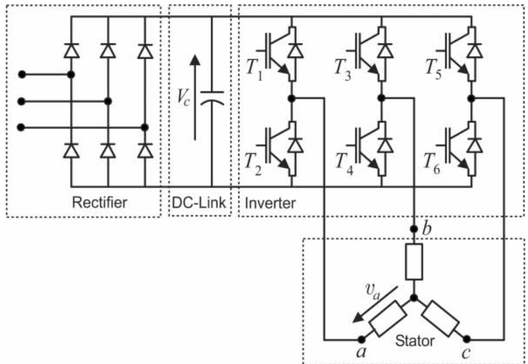

Figure 1. Power circuit of a three-phase voltage source two level inverter.

determined by the value of Y_1, Y_3 and Y_5 and they will be set together to form a binary number $Y_1 Y_3 Y_5$. Hence there are eight possible states.

2.2. *Voltage vectors*

The analysis below is based on the representation of machine variables by space vectors, the stator voltage space vector is defined by

$$\mathbf{v}_s = \frac{2}{3}\left(v_a + a v_b + a^2 v_c\right) \tag{1}$$

where $a = -(1/2) + (\sqrt{3}/2)j$. For the other three-phase variables, like flux and current, similar equations can be derived.

Of the eight inverter conduction states the combination 000 and 111 give the same result, zero phase voltage in all three phases, and clearly their space vector is $\mathbf{v}_s = 0$. The other six combinations are listed in table 1 and illustrated in figure 2.

3. Dynamic equations of the induction machine

The dynamic behaviour of the induction motor can be described by a set of differential equations of its space vector quantities. For the purposes of this work, it is advantageous to express them in a rotating frame of reference (index d for real part and q for imaginary part). Choosing the stator currents (i_{sd}, i_{sq}) and the rotor fluxes (ψ_{rd}, ψ_{rq}) as the state variables, the state equation of the induction machine

Vector	Value	State
$\mathbf{V}_1$	$(2/3)V_c$	100
$\mathbf{V}_2$	$2/3V_c\,e^{j(\pi/3)}$	110
$\mathbf{V}_3$	$2/3V_c\,e^{j(2\pi/3)}$	010
$\mathbf{V}_4$	$-(2/3)V_c$	011
$\mathbf{V}_5$	$2/3V_c\,e^{j(4\pi/3)}$	001
$\mathbf{V}_6$	$2/3V_c\,e^{j(5\pi/3)}$	101

Table 1. Voltage space vectors generated by the inverter.

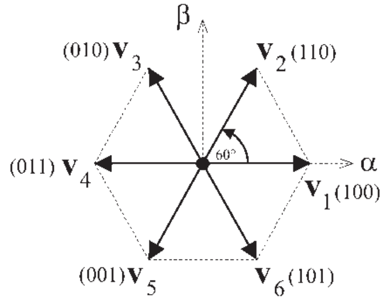

Figure 2. Voltage space vectors generated by a two level inverter.

can be expressed by

$$\frac{\mathrm{d}}{\mathrm{d}t}\begin{bmatrix} i_{sd} \\ i_{sq} \\ \psi_{rd} \\ \psi_{rq} \end{bmatrix} = \begin{bmatrix} -\bar{R}/(\sigma L_s) & \omega_{syn} & L_m R_r/(\sigma L_s L_r^2) & L_m \omega_r/(\sigma L_s L_r) \\ -\omega_{syn} & -\bar{R}/(\sigma L_s) & L_m \omega_r/(\sigma L_s L_r) & L_m R_r/(\sigma L_s L_r^2) \\ L_m R_r/L_r & 0 & -R_r/L_r & \omega_2 \\ 0 & L_m R_r/L_r & -\omega_2 & -R_r/L_r \end{bmatrix} \begin{bmatrix} i_{sd} \\ i_{sq} \\ \psi_{rd} \\ \psi_{rq} \end{bmatrix} + \begin{bmatrix} 1/(\sigma L_s) & 0 \\ 0 & 1/(\sigma L_s) \\ 0 & 0 \\ 0 & 0 \end{bmatrix} \begin{bmatrix} v_{sd} \\ v_{sq} \end{bmatrix} \tag{2}$$

where R_s and R_r are the stator and rotor resistances; L_s, L_r and L_m are the stator, rotor and mutual inductances and ω_r, ω_{syn} and ω_2 are the rotor mechanical speed, the electrical stator and rotor frequencies respectively (related by $\omega_r = \omega_{syn} - \omega_2$). In addition, σ is the total leakage factor defined by

$$\sigma = 1 - \frac{L_m^2}{L_s L_r} \tag{3}$$

and $\bar{R}$ is the stator equivalent resistance:

$$\bar{R} = R_s + \left(\frac{L_m^2}{L_r^2}\right) R_r. \tag{4}$$

Finally, the stator voltages (v_{sd}, v_{sq}) are the input variables of the system.

4. Current control in a rotating frame of reference

4.1. *Control strategy*

The state equations of the induction machine (2), are the basis in obtaining the block diagram shown in figure 3. Here, voltage v_{sd} and v_{sq}, generated by the inverter, are the variables used to control the state variables i_{sd} and i_{sq}. The terms depending on ψ_{rd}, ψ_{rq} and i_{sq} at the input of the first-order block ($K = 1/\bar{R}$, $\tau = \sigma L_s/\bar{R}$) of the d-axis in figure 3 are considered perturbations, from a control point of view.

One hysteresis controller is used to control current i_{sd}, while another controller is used to control the current in the other axis. Thus, the current control acts directly in a rotating frame of reference $d - q$.

The hysteresis element shown in figure 3 represent the action of the inverter and the current controllers. The output of each hysteresis element is directly the voltage generated by the inverter in the corresponding axis d or q. The width of the hysteresis in the d (q) axis is $2\delta_d$ ($2\delta_q$).

The d (q) current error ε_d (ε_q) is fed to the hysteresis, where if the error is positive and greater (smaller) than δ_d (δ_q) the output h_d (h_q) is 1 (0) and v_{sd} (v_{sq}) should

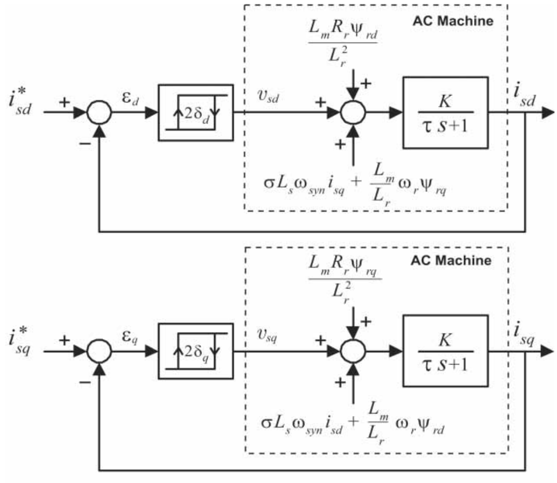

Figure 3. Control principle of the currents i_{sd} and i_{sq}.

increase (decrease). The current control strategy works as follows:

$$
\begin{array}{llll}
\text{if } \varepsilon_d > \delta_d, & \text{then } h_d = 1, & v_{sd} > 0 & \text{and current } i_{sd} \text{ increases} \\
\text{if } \varepsilon_d < -\delta_d, & \text{then } h_d = 0, & v_{sd} < 0 & \text{and current } i_{sd} \text{ decreases} \\
\text{if } \varepsilon_q > \delta_q, & \text{then } h_q = 1, & v_{sq} > 0 & \text{and current } i_{sq} \text{ increases} \\
\text{if } \varepsilon_q < -\delta_q, & \text{then } h_q = 0, & v_{sq} < 0 & \text{and current } i_{sq} \text{ decreases.}
\end{array}
$$

The next step is to find the relation between voltages v_{sd} and v_{sq} and the voltage vectors generated by the inverter.

4.2. *Voltage vector selection*

The complex plane is divided into six sectors shown in figure 4. Note that the sectors are limited by two contiguous inverter voltage space vectors, and that the rotating frame of reference is also included. For the current control it is important to detect the position of the rotating frame of reference. This will be done later.

Table 2 contains the voltage vector selection and the gate drive pulses for the transistors, depending on the hysteresis outputs and the sectors in which the d axis lays.

As an example, the case where the d axis is in sector 1 is explained (see figure 4):

- If the output of the current controllers are $h_d=0$ and $h_q=0$, this means that currents i_{sd} and i_{sq} must decrease. Thus, voltages v_{sd} and v_{sq} must be negative. The only inverter space vector accomplishing these conditions is $\mathbf{V}_5$.
- If the output of the current controllers are $h_d=0$ and $h_q=1$, this means that i_{sd} must decrease and i_{sq} must increase. Hence, voltage v_{sd} must be negative and v_{sq} must be positive. The only inverter space vector accomplishing these conditions is $\mathbf{V}_4$.
- If the output of the current controllers are $h_d=1$ and $h_q=1$, this means that i_{sd} and i_{sq} must increase. Hence, voltages v_{sd} and v_{sq} must be positive. The only inverter space vector accomplishing these conditions is $\mathbf{V}_2$.

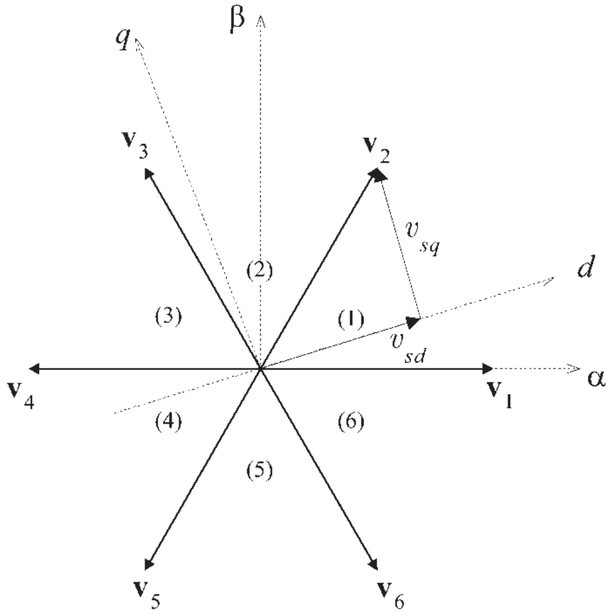

Figure 4. The complex plane divided in six sectors.

Sector	h_d	h_q	Vector	Inv. State
1	0	0	$\mathbf{V}_5$	001
1	1	0	$\mathbf{V}_1$	100
1	0	1	$\mathbf{V}_4$	011
1	1	1	$\mathbf{V}_2$	110
2	0	0	$\mathbf{V}_6$	101
2	1	0	$\mathbf{V}_2$	110
2	0	1	$\mathbf{V}_5$	001
2	1	1	$\mathbf{V}_3$	010
3	0	0	$\mathbf{V}_1$	100
3	1	0	$\mathbf{V}_3$	010
3	0	1	$\mathbf{V}_6$	101
3	1	1	$\mathbf{V}_4$	011
4	0	0	$\mathbf{V}_2$	110
4	1	0	$\mathbf{V}_4$	011
4	0	1	$\mathbf{V}_1$	100
4	1	1	$\mathbf{V}_5$	001
5	0	0	$\mathbf{V}_3$	010
5	1	0	$\mathbf{V}_5$	001
5	0	1	$\mathbf{V}_2$	110
5	1	1	$\mathbf{V}_6$	101
6	0	0	$\mathbf{V}_4$	011
6	1	0	$\mathbf{V}_6$	101
6	0	1	$\mathbf{V}_3$	010
6	1	1	$\mathbf{V}_1$	100

Table 2. Voltage vector selection look-up table for nonlinear current control.

- Finally, if the output of the current controllers are $h_d = 1$ and $h_q = 0$, this means that i_{sd} must increase and i_{sq} must decrease. Thus, voltage v_{sd} must be positive and v_{sq} must be negative. The only inverter space vector accomplishing these conditions is $\mathbf{V}_1$.

In this sector $\mathbf{V}_3$ and $\mathbf{V}_6$ are not used because its influence on the current behaviour changes according to the position of the d axis within sector 1. The same analysis holds for the remaining sectors.

4.3. *Speed control scheme*

The proposed current control method has been implemented as the internal loop of an indirect field oriented speed control of an induction machine, in a classical way, with imposed slip frequency (Trzynadlowski 2001, Kazmierkowski *et al.* 2002). Following this approach, when the rotating frame is oriented with the constant rotor flux ψ_r, the following relations are valid (Kazmierkowski *et al.* 2002)

$$T_e = K_2\omega_2 \tag{5}$$

$$i_{sq} = K_1\omega_2 \tag{6}$$

$$\theta_{syn} = \frac{1}{T}\int_0^t (\omega_r + \omega_2)\,\mathrm{d}t = \frac{1}{T}\int_0^t \omega_{syn}\,\mathrm{d}t \tag{7}$$

where K_1 and K_2 are proportional gains defined by the machine parameters (Kazmierkowski *et al.* 2002).

A simplified control diagram of the indirect field oriented control is illustrated in figure 5, where the proposed internal current control loop is highlighted. Note that this current control algorithm could also be implemented as part of a direct field oriented control scheme. Nevertheless, the simplicity of the indirect implementation has been privileged to show the feasibility of the proposed hysteresis current control.

The output of the speed proportional-integral controller delivers a magnitude proportional to the torque T_e and to the slip frequency ω_2 according to (5). This variable is multiplied by K_1 to obtain the reference value of current i_{sq}. The reference value of current i_{sd} is set to a constant value, which means operation with constant flux. The slip frequency ω_2 and the rotor speed ω_r are added and then integrated

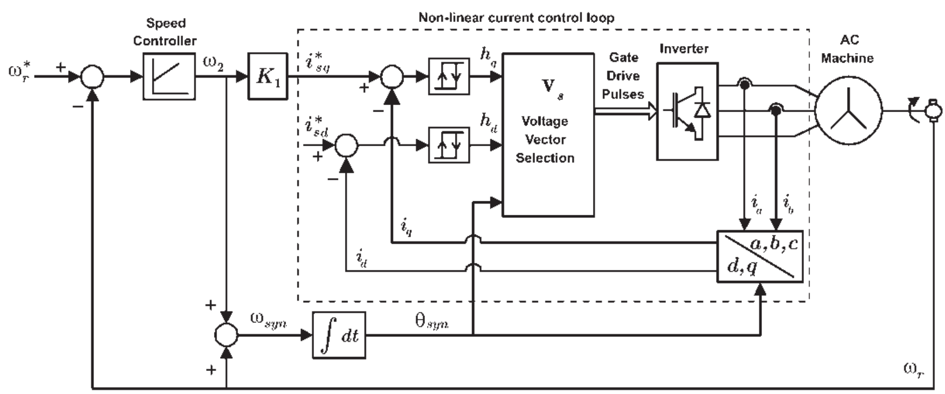

Figure 5. Simplified control scheme using nonlinear current control.

to obtain the position of the flux θ_{syn}. The output of the hysteresis controllers and the flux position θ_{syn} are used to address the look-up table, which delivers directly the gate drive pulses for the power transistors. The actual values of current i_{sd} and i_{sq} are obtained from the measured currents i_a and i_b, performing a vector rotation with the flux angle θ_{syn}.

5. Results

Experimental results have been obtained with a 4 kW 4-pole induction motor. Figure 6(*a*) shows the speed reversal of the drive from -1000 rpm to $+1000$ rpm. The overshoot present in the speed dynamic is produced by the tuning of the speed controller and is not relevant for the evaluation of the current control method.

The current response in control rotating reference frame is shown in figure 6(*b*) and (*c*). Here it can be seen that current i_{sq} reaches a maximum value of 47 A, which is limited at the output of the speed controller. It must be noted that current i_{sq} shows very fast dynamics without affecting the constant value of current i_{sd}, confirming the high quality of the current control in each axis. It can be observed that the load currents are quite sinusoidal.

6. Comparison with DTC

The basic principle and the most relevant features of DTC are presented in the Appendix for comparison purposes. It can be observed that the main speed control scheme proposed in this work (figure 5) and the one used by DTC (figure 7) have a very similar structure: one PI-controller for the speed and two hysteresis controllers for the rest of the variables.

While DTC uses a hysteresis comparator to control the torque, the proposed current control method uses it to control a current proportional to the torque (i_{sq}). On the other hand, the current control method studied in this paper uses a hysteresis comparator to control a current proportional to the rotor flux (i_{sd}), instead of using it to control directly the stator flux as done by DTC.

In addition, it can be observed that both methods generate similar look up tables, which means that they select the same voltage vectors. The main difference is that DTC works in polar coordinates (ψ_s, θ_s) and is oriented with the stator flux, while the current control works in cartesian coordinates (i_{sd}, i_{sq}) and is oriented with the rotor flux.

7. Conclusion

Both control methods, the hysteresis current control and DTC, have a common basis that is the space vector analysis of the inverter and the use of nonlinear controllers. In addition, both methods have a very similar structure and performance, which is evident from observing the block diagram of the control strategies and the voltage vector selection look-up tables respectively.

Both methods have the same advantages: they do not use an additional modulator and they do not need to adjust linear controllers. This method, like DTC, produces a very fast torque control and consequently, a high quality in the dynamic behaviour of the motor. They have also similar drawbacks, like

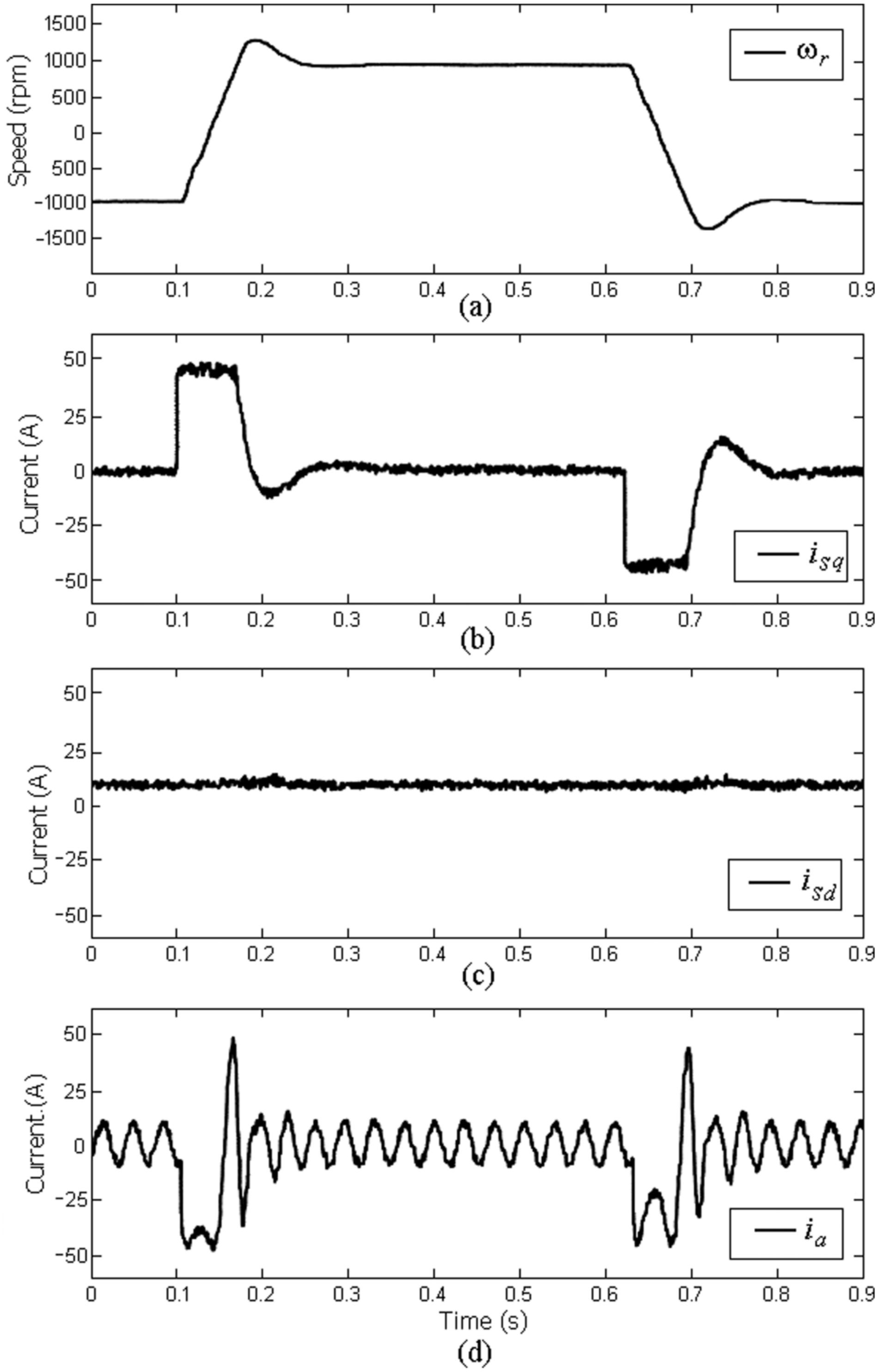

Figure 6. Speed reversal of a nonlinear current controlled Drive: (*a*) Drive mechanical speed ω_r; (*b*) Stator current i_{sq}; (*c*) Stator current i_{sd}; (*d*) Phase current i_a.

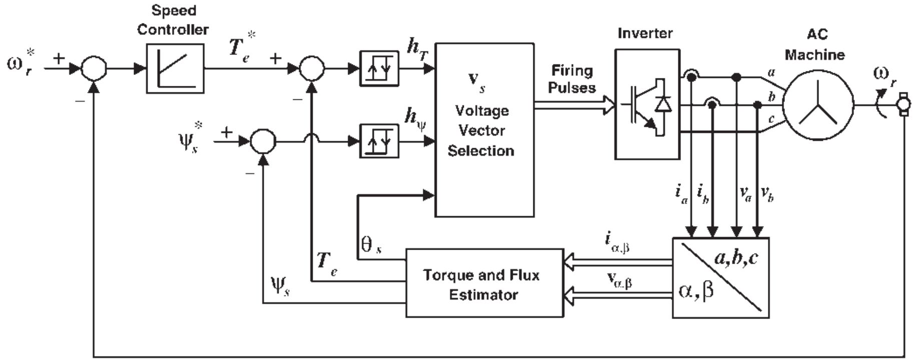

Figure 7. Simplified speed control scheme using DTC.

operations with variable switching frequency. This can be considered a problem in some applications.

However, both methods can operate with almost fixed switching frequency, by using more intelligent strategies proposed recently in the literature (Lee *et al.* 2002, Martins *et al.* 2002).

Finally, the authors hope that this work will contribute to enrich the variety of control methods used in inverter-fed motor drives.

Acknowledgment

The authors gratefully acknowledge the financial support provided by the Chilean National Scientific and Technological Development Fund (FONDECYT), under grant no. 1040183.

Appendix: basic principles of DTC

The stator flux vector ($\boldsymbol{\psi}_s$) of an induction machine is related to the stator voltage vector ($\mathbf{v}_s$) by (referred to in stator coordinates)

$$\frac{\mathrm{d}\boldsymbol{\psi}_s(t)}{\mathrm{d}t} = \mathbf{v}_s(t) - R_s \mathbf{i}_s. \tag{8}$$

Maintaining $\mathbf{v}_s$ constant over a sample time interval Δt and neglecting the stator resistance R_s, the integration of (8) yields to

$$\Delta\boldsymbol{\psi}_s(t) = \boldsymbol{\psi}_s(t) - \boldsymbol{\psi}_s(t-\Delta t) = \int_{t-\Delta t}^{t} \mathbf{v}_s(t)\,\mathrm{d}\tau = \mathbf{v}_s(t)\Delta t. \tag{9}$$

Equation (9) reveals that the stator flux vector is directly affected by variations on the stator voltage vector. On the contrary, the influence of $\mathbf{v}_s$ over the rotor flux is filtered by the rotor and stator leakage inductances, and is therefore not relevant over a short time horizon. Since the stator flux can be changed quickly while the rotor flux reacts slower, the angle between both vectors (θ_{sr}) can be controlled directly by $\mathbf{v}_s$. A graphical representation of the stator and rotor flux behaviour is illustrated in figure 8.

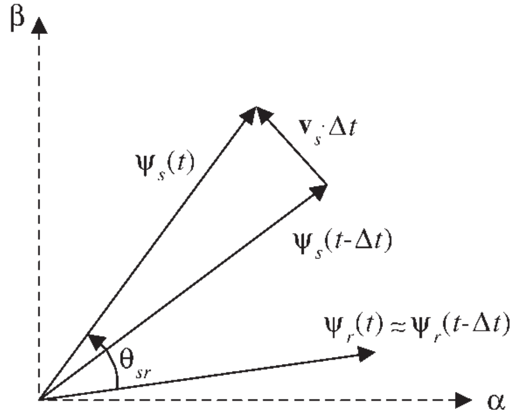

Figure 8. Influence of $\mathbf{v}_s$ over $\boldsymbol{\psi}_s$ during a sample interval Δt.

Since the electromagnetic torque developed by an induction machine (Novotny and Lipo 1996), is expressed by

$$T_e = \frac{3}{2}\frac{L_m}{L_\sigma^2} p \boldsymbol{\psi}_s \boldsymbol{\psi}_r \sin(\theta_{sr}) \tag{10}$$

it follows that the change in the angle θ_{sr} due to the action of $\mathbf{v}_s$ allows for direct and fast change in the developed torque T_e.

Direct torque control uses this principle to achieve the desired torque response of the induction machine, by applying the appropriate stator voltage vector to correct the flux trajectory (Mohan 2001).

A.1. *Voltage vector selection*

The task is to determine which voltage vector ($\mathbf{v}_s$) will correct the torque and flux response, knowing the torque and flux errors ($\varepsilon_\psi = \psi_s^* - \psi_s, \varepsilon_T = T_e^* - T_e$) and the stator flux vector position (sector determined by angle θ_s). Note that the next voltage vector applied to the load will always be one of the six vectors generated by the inverter.

Using (9) and (10), and analysing sector 1, for example, according to figure 9, the application of $\mathbf{V}_1$ increases the stator flux amplitude but reduces angle θ_{sr} which implies a reduction for T_e. On the contrary, $\mathbf{V}_4$ reduces the magnitude of $\boldsymbol{\psi}_s$, while it increases θ_{sr} and thus T_e. If $\mathbf{V}_2$ is applied to the load, both flux and torque increase, and it is clear that $\mathbf{V}_5$ produces the contrary effect. Note that $\mathbf{V}_3$ and $\mathbf{V}_6$ are not considered for selection in sector 1, because both change their influence over T_e, depending on which part of the sector $\boldsymbol{\psi}_s$ is located. The same analysis can be carried out for the other sectors. Table 3 summarizes the vector selection possibilities according to this criterion for the different sectors and hysteresis comparators output (or desired $\boldsymbol{\psi}_s$ and T_e corrections).

A.2. *Speed control scheme*

Figure 7 shows the basic cascade control diagram used for DTC. The outer loop controls the drive mechanical speed ω_r, while the inner loop corrects the electrical

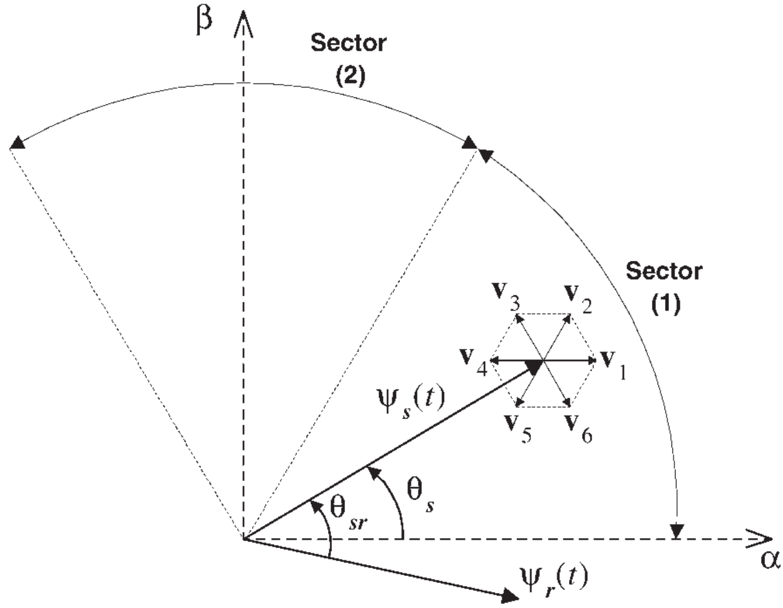

Figure 9. Illustration of voltage selection in sector 1.

Sector	h_ψ	h_T	Vector	Inv. State
1	0	0	$\mathbf{V}_5$	001
1	1	0	$\mathbf{V}_1$	100
1	0	1	$\mathbf{V}_4$	011
1	1	1	$\mathbf{V}_2$	110
2	0	0	$\mathbf{V}_6$	101
2	1	0	$\mathbf{V}_2$	110
2	0	1	$\mathbf{V}_5$	001
2	1	1	$\mathbf{V}_3$	010
3	0	0	$\mathbf{V}_1$	100
3	1	0	$\mathbf{V}_3$	010
3	0	1	$\mathbf{V}_6$	101
3	1	1	$\mathbf{V}_4$	011
4	0	0	$\mathbf{V}_2$	110
4	1	0	$\mathbf{V}_4$	011
4	0	1	$\mathbf{V}_1$	100
4	1	1	$\mathbf{V}_5$	001
5	0	0	$\mathbf{V}_3$	010
5	1	0	$\mathbf{V}_5$	001
5	0	1	$\mathbf{V}_2$	110
5	1	1	$\mathbf{V}_6$	101
6	0	0	$\mathbf{V}_4$	011
6	1	0	$\mathbf{V}_6$	101
6	0	1	$\mathbf{V}_3$	010
6	1	1	$\mathbf{V}_1$	100

Table 3. Voltage vector selection look-up table for DTC.

torque dynamics using DTC principle. The torque and stator flux errors are controlled by the hysteresis comparators, whose outputs together with the stator flux vector position (θ_s) access the appropriate voltage vector ($\mathbf{v}_s$) of the look-up table. Once the voltage vector is chosen, the corresponding gate drive pulses are delivered to the inverter semiconductors. The inverter generates the selected voltage vector and torque correction is achieved.

Finally, the drive measured variables v_a, v_b, i_a and i_b are transformed to α–β coordinates to estimate T_e, $\boldsymbol{\psi}_s$ and θ_s for feedback purposes.

This basic DTC scheme works with variable switching frequency, which is not very attractive in several applications. A number of advances, like switching frequency imposition and use of three-valued hysteresis comparators for torque control, have improved the behaviour of DTC (Lee *et al*. 2002, Martins *et al*. 2002).

References

Boldea, I., and Nasar, S., 1999, *Electric Drives* (Boca Raton, FL: CRC Press LLC).

Depenbrock, M., 1988, Direct selfcontrol (DSC) of inverter-fed induction machine. *IEEE Transactions on Power Electronics*, **3**, 420–429.

Kazmierkowski, M., Krishnan, R., and Blaabjerg, F., 2002, *Control in Power Electronics: Selected Problems* (San Diego, CA: Academic Press).

Lee, K., Song, J.,Choy, I., and Yoo, J., 2002, Torque ripple reduction in DTC of induction motor driven by three-level inverter with low switching frequency. *IEEE Transactions on Power Electronics*, **17**, 255–264.

Martins, C., Roboam, X., Meynard, T., and Carvalho, A., 2002, Switching frequency imposition and ripple reduction in DTC drives by using a multilevel converter. *IEEE Transactions on Power Electronics*, **17**, 286–297.

Mohan, N., 2001, *Advanced Electric Drives: Analysis, Control and Modeling Using Simulink* (Minneapolis: MNPERE).

Novotny, D., and Lipo, T., 2006, *Vector Control and Dynamics of AC Drives* (New York: Oxford University Press).

Rodríguez, J., and Kastner, G., 1985, A forced commutated cycloconverter for three-phase load with control of source and load currents. *Proceedings for 1st European Conference on Power Electronics EPE*, **85**, 1141–1146.

Rodríguez, J., and Kastner, G., 1987, Nonlinear current control of an inverter-fed induction machine. *ATZ Archiv*, **9**, 250–254.

Takahashi, I., and Noguchi, T., 1986, A new quick-response and high-efficiency strategy of an induction motor. *IEEE Transactions on Industry Applications*, **22**, 820–827.

Tiitinen, P., Pohjalainen, P., and Lalu, J., 1995, The next generation motor control method: direct torque control (DTC). *EPE Journal*, **5**, 14–18.

Trzynadlowski, A., 2001, *Control of Induction Motors* (San Diego, CA: Academic Press).

Vas, P., 1998, *Sensorless Vector and Direct Torque Control* (New York: Oxford University Press).